Copolyesters of Poly(ethylene terephthalate), Hydroquinone Diacetate, and Terephthalic Acid: A Simple Rate Model for Catalyzed Synthesis in the Melt†

J. Mathew, R. S. Ghadage, A. Lodha, and S. Ponrathnam*

Polymer Science and Engineering Group, Chemical Engineering Division, National Chemical Laboratory, Pune 411 008, India

S. D. Prasad*

Physical Chemistry Division, National Chemical Laboratory, Pune 411 008, India

Received June 15, 1995; Revised Manuscript Received July 25, 1996⊗

ABSTRACT: The kinetics of melt transesterification between poly(ethylene terephthalate) (PET), hydroquinone diacetate (HQDA), and terephthalic acid (TA) is examined. The considerably complex system is treated by methods analogous to solution kinetics. A number of assumptions are proposed and validated to simplify the kinetics and to make the analysis tractable. A key postulation is that the reaction originates between HQDA and TA to form a dimer which slices the PET chain. The subsequent coupling of segments re-forms the PET chain with random incorporation of HQDA−TA units. The steady−state approximation is invoked for the rate of generation of dimer. The number of moles of acetic acid, generated in both homopolyesterification (HQDA−TA) and copolyesterification (coupling of segments) channels, is monitored to follow the overall rate of the reaction and to evaluate the individual rate constants. The rate constants obtained for a majority of compositions conform to that predicted theoretically. The kinetic analysis reveals the implicit simplicity of complex systems.

Introduction

A global inquisition of the structure−property relationships in thermotropic liquid crystalline polymers (LCPs) evinces that the distinctiveness of the bridging groups in the mesogenic core and their directional effects dictate a number of significant thermal features like transition temperatures, the temperature range of thermotropic stability (mesogenic gap), etc.[1−7]

The structural organizations in the thermotropic liquid crystalline aromatic copolyesters are well documented.[8−15] These are specifically synthesized through copolyesterification to tailor-make structures which elicit the desired properties. Copolyesterification helps in imparting definite physicochemical properties to the system attributable to the major component. The major component principally consists of benzene rings fastened exclusively at para positions by ester groups and may be present as sequences of either 4-oxybenzoate or 1,4-oxyphenyleneoxy and 1,4-carbonyloxyphenylenecarbonyloxy units. The parent polyesters of the major components are so high melting (>600 °C) that degradation precedes melting. A recourse to copolyesterification is sought, with the incorporation of flexible moieties,[8,9] rigid kinks, or substitution in the mesogenic core,[16−18] to induce a dramatic decline in transition temperature without a discernible compromise in the mechanical properties.

The PET−OB copolyester is formed by the transesterification between poly(ethylene terephthalate) and 4-acetoxybenzoic acid. This classic case of downward shift in transition temperature, induced through aliphatic flexible moieties, displays thermotropic character within a definite range of copolyester composition.[9] Transesterification reaction between poly(ethylene terephthalate), HQDA, and TA generates a system which differs from PET−OB only in the direction of the ester bridging group in the mesogenic core. This, however, alters the mechanical performance as well as solubility.[19] The reaction pathways in this three-component (PET−HQDA−TA) system ought to be intricate vis-à-vis that for the PET−OB system. The underlying reaction mechanisms in the catalyzed melt transesterification of a ternary nonthermotropic system from PET, 4,4′-isopropylidenediphenyl diacetate, and TA have been reported.[20]

There has been no evidence of kinetic explorations of the melt transpolyesterifications of the binary HQDA−TA system or the ternary PET−HQDA−TA system. An earlier inquiry relating to the copolyesterification of PET and 4-acetoxybenzoic acid did not manifest precipitation of poly(4-oxybenzoate).[21] The experimental kinetic data could be appropriately fitted using a second-order kinetic model. The present investigation forms a logical sequel. Here we explore the kinetics of the three-component system wherein a number of parallel reactions occur concurrently. As a prelude, we examine the binary HQDA−TA system.

The investigations were conducted with the following objectives: (1) to identify plausible routes to simplify the kinetics of a three-component system; (2) to determine the kinetic order with respect to the polyester of HQDA and TA as well as the copolyester of PET, HQDA, and TA; (3) to predict the rates of acetic acid generated in the HQDA−TA and PET−HQDA−TA systems; (4) to check whether precipitation of the polycondensate of HQDA−TA constitutes an added complication.[22]

The work is presented as follows: A simple reaction sequence is suggested to outline the dominant steps involved. Crucial reactions, which lead to acetic acid production, are taken into account in the kinetic analysis. Simple second-order kinetics is found to be effective for each of the steps significant to the acetic acid production. Finally, a steady-state assumption is invoked to make the analysis intelligible, since the network is nonlinear (consecutive parallel second-order

* To whom correspondence should be addressed.
† NCL Communication No. 5733.
⊗ Abstract published in *Advance ACS Abstracts,* February 1, 1997.

S0024-9297(95)00842-4 CCC: $14.00

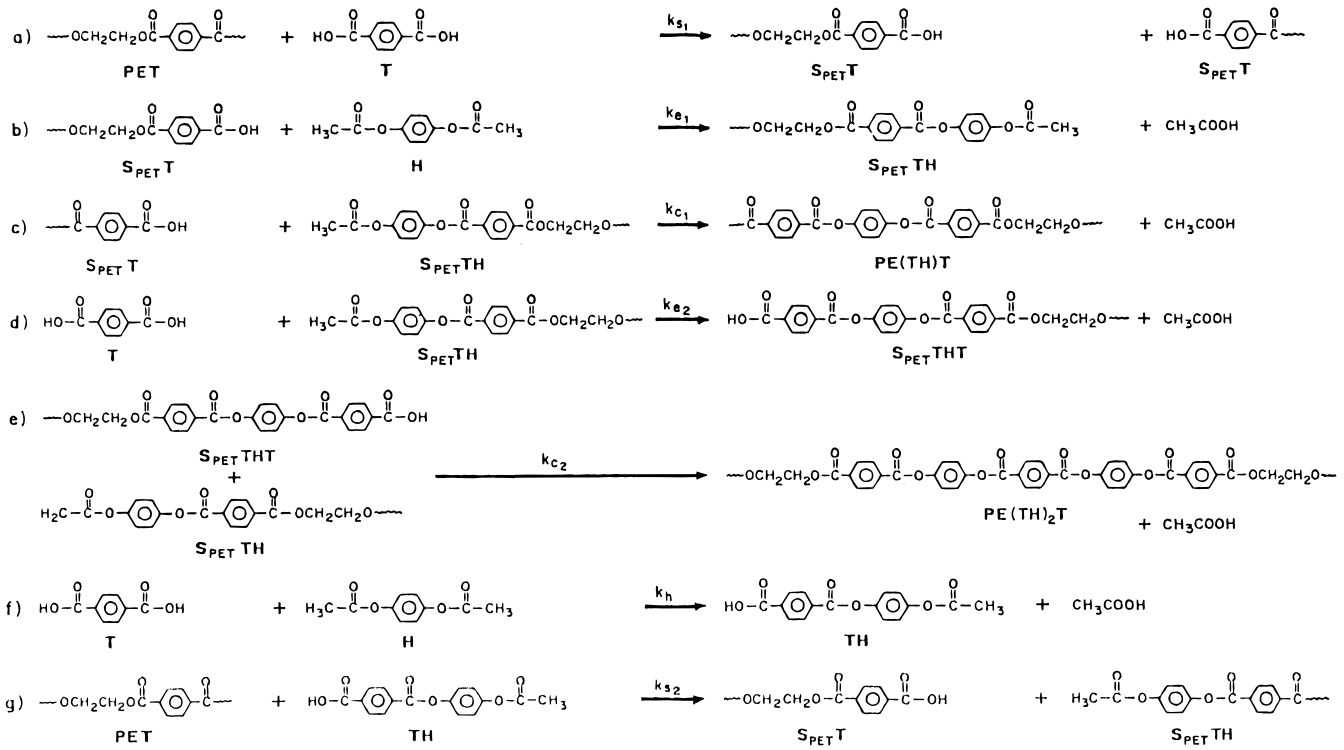

Figure 1. Mechanism of PET−HQDA−TA copolyesterification.

reactions). The correctness of this procedure is justified by experimental observations. Finally, physicochemical characteristics of the homo- and copolyesters are considered.

Experimental Section

Materials. Virgin, commercial fiber grade poly(ethylene terephthalate) (PET) with 2-hydroxyethyl end groups, manufactured from dimethyl terephthalate and ethylene glycol, of inherent viscosity 0.58 and 1678 μm particle size (M/S Century Enka Ltd., Pune, India) and purified terephthalic acid (TA) were used as received. The metal impurities originating from catalyst residues in PET and TA were estimated by atomic absorption spectrometry to be less than 10 ppm. HQDA was prepared by sulfuric acid catalyzed reaction of hydroquinone and acetic anhydride and was recrystallized from methanol. The product yield was 90% and the product had a melting point of 121 °C.

Reactor Fabrication. A 250 mL, glass-lined, electrically heated reactor,[22] previously described, was used for the melt transesterification.

Preparation of Polyesters. The transesterifications were conducted with the objective of analyzing the copolyesterification kinetics in the initial stages of the reaction wherein the distillation of the byproduct, acetic acid, was completed under atmospheric pressure. Transesterifications were conducted to generate a series of copolyesters of varying compositions. First, polyesterification of HQDA and TA was carried out at 50 mol % composition of each monomer. Then the transesterification kinetics of the copolyesterification were studied. Melt polyesterification kinetics of four compositions, PET 30/70 (HQDA + TA), PET 40/60 (HQDA + TA), PET 50/50 (HQDA + TA), and PET 60/40 (HQDA + TA), were studied, wherein 30:35:35, 40:30:30, 50:25:25, and 60:20:20 mol % of PET, HQDA, and TA were used.

PET melted around 256 °C and degraded when maintained isothermally for 15 min at 320 °C under atmospheric pressure. The isothermal reaction temperatures chosen for the kinetic estimations were 260, 275, 290, and 305 °C. A dry nitrogen blanket was maintained throughout the experiments to prevent oxidative degradations. The rate of evolution of byproduct, acetic acid, was monitored volumetrically to estimate the kinetic parameters. Dibutyltin oxide (0.1 mol % of HQDA) was used as catalyst for the melt transesterification reactions. The HQDA lost due to sublimation was monitored and was found to be less than 0.075 mol % of that charged. This implies that we do not have to make corrections in the overall mass balance for the HQDA lost. The purity of acetic acid formed was also estimated at different isothermal kinetic temperatures. This was found in general to be 94% at 275 °C and 92% at 290 and 305 °C, respectively. The formation of other volatile side products in low concentrations (<5%) is obviously a result of decarboxylation and etherification reactions.[23] Similarly, formation of a small amount of ethylene diacetate is also reported in the reaction of PET with 4,4′-isopropylidenediphenyl diacetate and TA.[20] Maximum conversion, noted on the basis of acetic acid generated, was around 80%. The reactions were then continued further under 0.05 Torr for 2 h to complete the polyesterifications. The reactants were charged out in the molten state and cooled to room temperature. The light tan and opaque homo- and copolyesters were powdered and extracted with sodium bicarbonate solution and methanol to remove the unreacted TA and HQDA prior to the characterization.

Measurements. The homo- and copolyesters were observed under a polarizing microscope equipped with a Koffler hot stage. A small amount of polyester was mounted between a slide and cover slip on the stage and heated at a constant rate. The polyesters were observed under crossed polarizers.

Thermal transitions were obtained with a Mettler DSC-30 apparatus interfaced with a thermal analysis data station under a nitrogen atmosphere using a sample size of 10−15 mg. A heating rate of 20 °C/min was employed in all cases. Indium was used to calibrate the enthalpy values. A trimetal (In−Pb−Zn) was used to calibrate the temperature scale. Samples were analyzed in the temperature range of 50−450 °C in the first and second heating cycles.

Results and Discussion

The reactions which occur when PET, HQDA, and TA are heated together or maintained isothermally at temperatures in excess of the isotropization temperature of crystalline PET may by visualized as shown in Figure 1. PET chain cleavage occurs principally through the

step represented in Figure 1a. PET chain cleavage with TA (T) results in the formation of two PET segments of similar or differing chain lengths but terminated with the carboxylic acid end group (TA end group) ($S_{PET}T$), as per the mechanism described earlier for cleavage of PET with TA on the basis of the experimental observation of the reaction between PET−TA and PET−4,4′-isopropylidenediphenyl diacetate, respectively.[20] Viscosity measurements indicated that while TA slices PET, this does not proceed with 4,4′-isopropylidenediphenyl diacetate. In the present study, reaction between PET and HQDA did not lead to a decrease in the viscosity of PET. The rate of this reaction is far too slow to be of any significance to the overall process under consideration here.[24] Acetic acid is not generated during the slicing of PET by TA. This should be borne in mind in computing its generation rate.

The $S_{PET}T$ segment reacts with HQDA (H) to form PET segment $S_{PET}TH$ terminated with the acetoxy end group (hydroquinone end group) and generates acetic acid as depicted in Figure 1b. The segment $S_{PET}T$ and segment $S_{PET}TH$ could then react to re-form the PET chain with the insertion of the hydroquinone−terephthalate unit and the generation of acetic acid as presented in Figure 1c. The other possible reactions of these segments are also shown in Figure 1d,e. The other inherent major reaction pathways are (i) transesterification of HQDA and TA to form hydroquinone−terephthalate (Figure 1f) and (ii) the insertion of the hydroquinone−terephthalate unit into the PET chain (Figure 1g,c) as per the mechanism described for insertion of oxybenzoate into the PET chain.[21] These major reactions are shown below.

$$\text{PET} + \text{T} \xrightarrow{k_{s_1}} 2\text{S}_{\text{PET}}\text{T} \qquad \text{(I)}$$

$$\text{S}_{\text{PET}}\text{T} + \text{H} \xrightarrow{k_{e_1}} \text{S}_{\text{PET}}\text{TH} + \text{CH}_3\text{COOH} \qquad \text{(II)}$$

$$\text{S}_{\text{PET}}\text{TH} + \text{S}_{\text{PET}}\text{T} \xrightarrow{k_{c_1}} \text{PE(TH)T} + \text{CH}_3\text{COOH} \qquad \text{(III)}$$

$$\text{T} + \text{S}_{\text{PET}}\text{TH} \xrightarrow{k_{e_2}} \text{S}_{\text{PET}}\text{THT} + \text{CH}_3\text{COOH} \qquad \text{(IV)}$$

$$\text{S}_{\text{PET}}\text{THT} + \text{S}_{\text{PET}}\text{TH} \xrightarrow{k_{c_2}} \text{PE(TH)}_2\text{T} + \text{CH}_3\text{COOH} \qquad \text{(V)}$$

$$\text{T} + \text{H} \xrightarrow{k_h} \text{TH} + \text{CH}_3\text{COOH} \qquad \text{(VI)}$$

$$\text{PET} + \text{TH} \xrightarrow{k_{s_2}} \text{S}_{\text{PET}}\text{T} + \text{S}_{\text{PET}}\text{TH} \qquad \text{(VII)}$$

Here, k_s (k_{s_1}, k_{s_2}), k_e (k_{e_1}, k_{e_2}), k_c (k_{c_1}, k_{c_2}), and k_h are the rate constants of chain slicing, chain extension, copolyesterification, and transesterification, respectively. Subscripts 1 and 2 represent the different modes of reaction. We now add up reaction schemes I, II, and III. The result is the overall reaction givin by eq VIII.

$$\text{PET} + \text{T} + \text{H} \rightarrow \text{PE(TH)T} + 2\text{CH}_3\text{COOH} \qquad \text{(VIII)}$$

A similar expression can also be obtained by combining eqs VI, VII, and III, as shown in eq IX.

$$\text{PET} + \text{T} + \text{H} \rightarrow \text{PE(TH)T} + 2\text{CH}_3\text{COOH} \qquad \text{(IX)}$$

Equations VIII and IX are identical, but the ways they are formed are different. In eq VIII insertion of the hydroquinone−terephthalate (TH) unit into PET is the resultant of three reaction sequences: (a) PET chain cleavage by TA to form $S_{PET}T$, (b) $S_{PET}T$ segment extension by HQDA to form $S_{PET}TH$, and (c) coupling of segments $S_{PET}T$ and $S_{PET}TH$, resulting in the insertion of the hydroquinone−terephthalate unit into the PET chain. In the case of eq IX, insertion of TH is visualized as (a) dimerization of HQDA and TA to form TH, (b) PET chain cleavage by dimer TH to generate segments $S_{PET}T$ and $S_{PET}TH$, and (c) coupling of segments $S_{PET}T$ and $S_{PET}TH$, resulting in the insertion of the hydroquinone−terephthalate unit into the PET chain.

Reaction schemes IV and V are considered only to show how larger blocks of TH units are inserted into the PET chain. These reactions are feasible only if the concentrations of HQDA and TA are in excess of 67%. Reaction events IV and II are equivalent. Here the reactions are between PET segment and a monomer. Similarly, reaction scheme V is identical to reaction scheme III, i.e. re-formation of the PET chain with the insertion of the TH unit due to the reactions between two PET segments. Therefore, reactions I−III, VI, and VII are the dominant reactions. There are two possible pathways through which the TH unit can be inserted into the PET chain, as described earlier. These two mechanisms are based on the combination of eqs I, II, and III and eqs VI, VII, and III, respectively. This clearly indicates that eq III is common for both mechanisms. Hence, there is the principal reaction event which is between $S_{PET}T$ and $S_{PET}TH$ leading to the formation of the PET chain with the insertion of the hydroquinone−terephthalate unit. This is the only reaction path leading to copolyesterification. Therefore, generation of such segments is important as far as copolyesterification is concerned. According to the mechanism based on PET chain cleavage by TA, these segments ($S_{PET}T$ and $S_{PET}TH$) are generated by reaction schemes I and II. On the contrary, these segments are formed in a single-step reaction (eq VII) as per the mechanism based on PET chain cleavage by the TH dimer.

Thus, one can visualize the existence of many variables (rate constants) for these independent reactions. It is a difficult task to analytically solve for these kinetic variables. Hence the following assumptions are made to simplify the kinetic picture: (1) The reaction between HQDA and TA leads to the formation of dimers (TH). (2) An oligomer (dimer) of HQDA and TA can cleave the PET chain to form PET segments $S_{PET}T$ and $S_{PET}TH$. (3) These segments then reat to re-form the PET chain with insertion of the TH moiety. Hence, the reactions leading to the copolyester of interest are given by eqs A and B.

Formation of the copolyester proceeds by a mechanism outlined below:

If c denotes the dimer formed by the reaction of HQDA and TA, then the following steps can be presumed for the copolyesterification reactions.

$$\underset{(a-x)}{\text{H}} + \underset{(a-x)}{\text{T}} \xrightarrow{k_1} \underset{(c)}{\text{TH}} + \underset{(x+y)}{\text{CH}_3\text{COOH}} \qquad \text{(A)}$$

$$\underset{(q-y)}{\text{PET}} + \underset{(c)}{\text{TH}} \xrightarrow{k_2} \underset{(y)}{\text{PE(TH)T}} + \underset{(x+y)}{\text{CH}_3\text{COOH}} \qquad \text{(B)}$$

where H, T, TH, PET, PE(TH)T, CH_3COOH, a, c, x, y, and q denote HQDA, TA, dimer of HQDA and TA, poly(ethylene terephthalate), copolyester, acetic acid, initial

concentration of HQDA and TA, concentration of dimer, number of moles of HQDA or TA converted, number of moles of PET segments converted, and initial concentration of PET, respectively. k_1 and k_2 denote the rate constants of polyesterification and copolyesterification, respectively. Equation B is the resultant of eqs VII and III. These two reactions are combined because segments $S_{PET}T$ and $S_{PET}TH$ are formed through eq VII without generating acetic acid and are reunited to reform the PET chain with insertion of the TH unit as per eq III. The rate of formation of the dimer can be given as

$$\frac{dx}{dt} = -\frac{d[H]}{dt} = -\frac{d[T]}{dt} = k_1(a-x)^2 \qquad (1)$$

The rate of formation of the copolyester can be given as

$$\frac{dy}{dt} = -\frac{d[PET]}{dt} = k_2 c(q-y) \qquad (2)$$

$$\frac{dc}{dt} = k_1(a-x)^2 - k_2 c(q-y) \qquad (3)$$

The total rate of acetic acid production is given by the algebraic sum of eqs 1 and 2. The total rate of acetic acid formation can be given by

$$\frac{d[CH_3COOH]}{dt} = \frac{dx}{dt} + \frac{dy}{dt} = k_1(a-x)^2 + k_2 c(q-y) \qquad (4)$$

Equation 1 can be integrated to give x as a function of time

$$\frac{1}{a-x} - \frac{1}{a} = k_1 t \qquad (4a)$$

One can substitute for $(a - x)$ found from eq 4a in eqs 3 and 4. However, what is measured experimentally is $(x + y)$ moles of acetic acid produced and not x or y individually. While eq 1 is readily integrable, c in eq 2 has to be expressed in terms of x and y before we can integrate it. But from conservation of residues of H and T (molecular entities minus the reactive end groups), we have

$$x = c + y \qquad (5a)$$

or

$$c = x - y \qquad (5b)$$

Equation 2 now becomes

$$\frac{dy}{dt} = k_2(x-y)(q-y) \qquad (6)$$

Equation 6 is not integrable as it is quadratic in y and has a complex nonlinear dependence on t. However, a numerical procedure, which is otherwise warranted, is not employed. Later it will be seen that a simple closed form of kinetic expression is sufficient to correlate the experimental data.

A Simplified Kinetic Picture. The reaction between HQDA and TA is slow. Cleavage of PET by TA does not generate acetic acid as seen from eq I. Thus, the rate of formation of the dimer (c) is rate controlling for the generation of acetic acid. The subsequent incorporation of c into the polyester through PET chain slicing and the recombination of segments are so fast that effectively the steady-state concentration of c will be very small. Also, the rate of production of dimer can be set equal to zero.

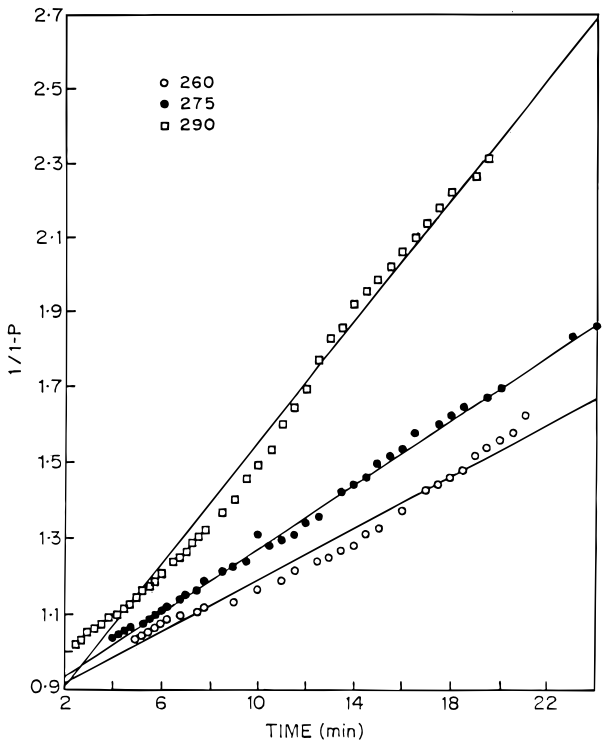

Figure 2. Second-order plot illustrating effect of temperature for the HQDA−TA system (uncatalyzed reactions).

$$\frac{dc}{dt} = k_1(a-x)^2 - k_2(x-y)(q-y) = 0 \qquad (7)$$

and then

$$\frac{d(x+y)}{dt} = \frac{d[CH_3COOH]}{dt} = 2k_1(a-x)^2 \qquad (8)$$

Thus, the rate of production of acetic acid becomes equal to twice that of the previous case, where PET is absent (see eq 1).

Figure 2 shows a second-order plot which is indeed followed quite generally for the uncatalyzed HQDA and TA system at three different temperatures. Figure 3 indicates that the reaction rate is adequately modeled by second-order kinetics even for catalyzed reactions. It is seen from plots in Figures 2 and 3 that the difference between them is mainly quantitative. If we attribute a physical meaning to $1/(1-p)$ as the number-average degree of polymerization $\overline{DP}$, it is obvious from the plots that the catalyst (dibutyltin oxide) does not play a major role in increasing the $\overline{DP}$. A glance at Table 1 reveals that the catalyst plays only a marginal role except for the first two compositions of 0 and 30% PET. At increasing PET compositions, the activation energies are almost identical within experimental uncertainty. This, in turn, is reflected in the values of the rate constants and activation energies. However, one particular composition having 30 mol % PET shows an anomaly. Even though the rate constants vary only marginally, except for 305 °C, the activation energy for the catalyzed reaction is almost twice. This is also apparent from Figure 4, where the least-squares fits for the Arrhenius plots are given for both uncatalyzed and catalyzed reactions. The error bars are also given. It is obvious that the plots are good and the error bars are within the limits of statistical variability associated

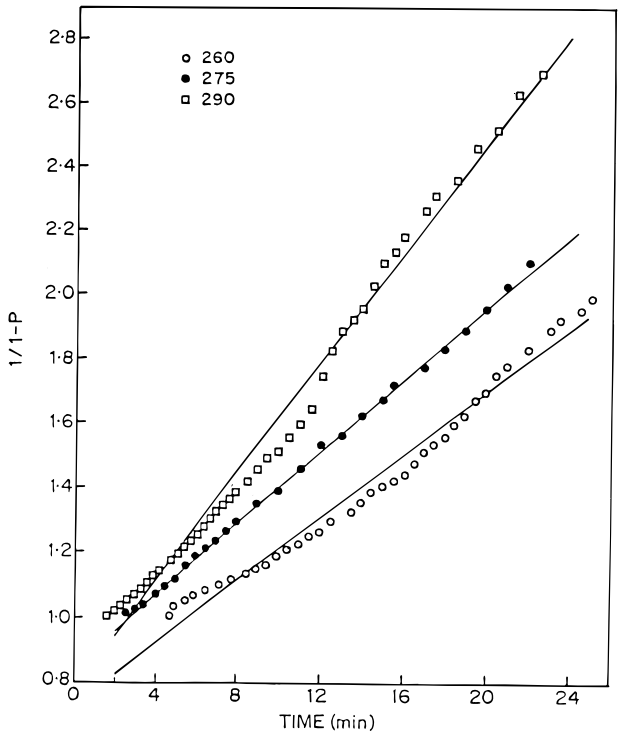

Figure 3. Second-order plot illustrating effect of temperature for the HQDA−TA system (catalyzed reactions).

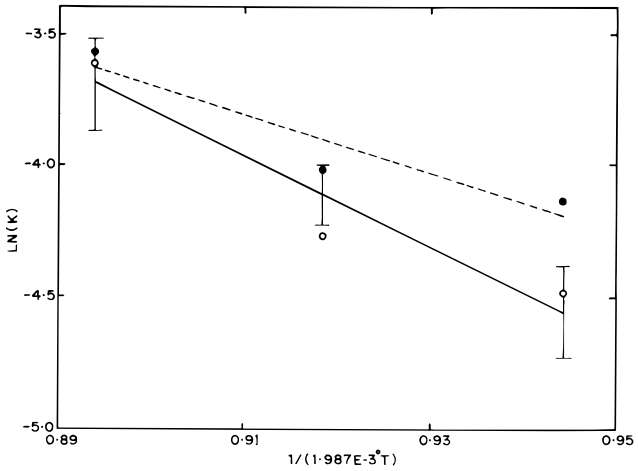

Figure 4. Arrhenius plot for uncatalyzed and catalyzed HQDA−TA reactions. Dashed and solid lines represent least-squares fit for catalyzed and uncatalyzed reactions, respectively. The error bars for the uncatalyzed reactions are only shown for clarity.

with just a few degrees of freedom. This is because only three temperatures are available for experimentation. The copolyesterification reaction between PET, HQDA, and TA was carried out at 260, 275, 290, and 305 °C. Figures 5−8 indicate that second-order kinetics is most generally followed by both catalyzed and uncatalyzed reactions at all compositions. A comparison of the uncatalyzed and catalyzed plots depicts that the difference between them is only quantitative. No breaks or large induction period is present. There is no appreciable improvement in the average degree of polymerization, as is noticed from the catalyzed reactions. Table 1 shows that there is no significant improvement in the rates of catalyzed reactions. The rate constant values show no trend with rise in PET mole percent, indicating that the copolyesterification mechanism remains independent of composition (PET:HQDA/TA mole ratio).

The validity of the steady-state assumption in the case of a copolyesterification reaction involving PET holds good. Rate constants in Table 1 indeed suggest that this is true in general. The numerical value of the rate constants, in particular, is equal to twice that observed for the HQDA/TA reaction. A few runs however show that this rate is slightly lower than two for the reaction at lower temperature. Qualitatively, it may be stated that the high melt viscosity of PET at low temperature might cause this lowering of reaction rates.

Before we discuss the temperature variation of the rate constants, a few remarks are in order regarding the role of diffusion, which can sometimes mask the true activation energies. It is common knowledge that melt phase viscosities are fairly high and in the Stokes−Einstein picture of diffusion, the diffusivities are inversely proportional to the viscosity. However, a noticeable manifestation of diffusional intrusion will be that the Arrhenius plots will have breaks at higher temperatures and there will be a lowering of the observed activation energy (slope) after the break signaling the transition to a diffusion-controlled regime.[25] We do not observe such behavior in any of our Arrhenius plots, signifying that such a complication does not arise. Besides, the bounds of activation energy (95% confidence interval, from a *t*-distribution with appropriate degrees of freedom) computed, do not allow for such an event.

Table 1. Rate Constants from Second-Order Plots of HQDA−TA and PET−HQDA−TA Systems

system	comp	temp (°C)	uncat. rate constant (L mol^{-1} s^{-1})	cat. rate constant (L mol^{-1} s^{-1})	uncat. EOA[a] (kcal/mol)	cat. EOA[a] (kcal/mol)
HQDA−TA	50−50	260	0.0113 ± 0.001	0.016 + 0.0012		
		275	0.014 ± 0.0004	0.018 ± 0.004	17.23 ± 5.35	11.06 ± 3.89
		290	0.027 ± 0.0012	0.028 ± 0.0014		
PET−HQDA−TA	30−35−35	260	0.018 ± 0.0014	0.011 ± 0.001		
		275	0.032 ± 0.0025	0.033 ± 0.003		
		290	0.050 ± 0.0028	0.044 ± 0.002	15.13 ± 3.17	27.63 ± 4.07
		305	0.053 ± 0.0025	0.095 ± 0.01		
PET−HQDA−TA	40−30−30	260	0.0210 ± 0.001	0.022 ± 0.0005		
		275	0.0335 ± 0.003	0.039 ± 0.0033		
		290	0.069 ± 0.005	0.0505 ± 0.004	18.73 ± 3.75	18.16 ± 1.81
		305	0.072 ± 0.005	0.089 ± 0.006		
PET−HQDA−TA	50−25−25	260	0.025 ± 0.001	0.024 ± 0.001		
		275	0.029 ± 0.001	0.027 ± 0.002		
		290	0.045 ± 0.002	0.049 ± 0.003	13.06 ± 1.83	14.40 ± 2.63
		305	0.063 ± 0.004	0.064 ± 0.004		
PET−HQDA−TA	60−20−20	260	0.017 ± 0.0007	0.020 ± 0.0012		
		275	0.036 ± 0.0008	0.041 ± 0.002		
		290	0.044 ± 0.01	0.046 ± 0.002	12.62 ± 4.73	10.55 ± 4.78
		305	0.044 ± 0.003	0.045 ± 0.004		

[a] EOA = energy of activation.

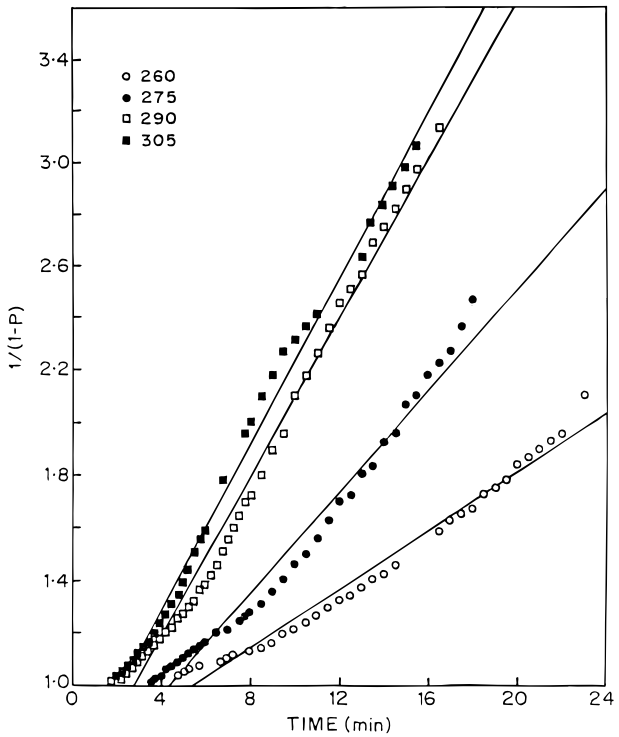

Figure 5. Second-order plot illustrating effect of temperature for uncatalyzed PET 30/70 (HQDA + TA) reactions.

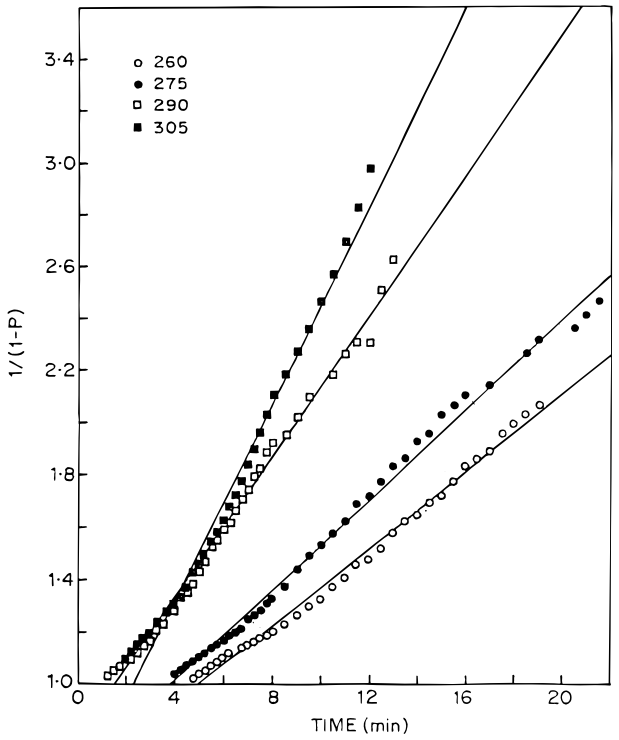

Figure 6. Second-order plot illustrating effect of temperature for uncatalyzed PET 50/50 (HQDA + TA) reactions.

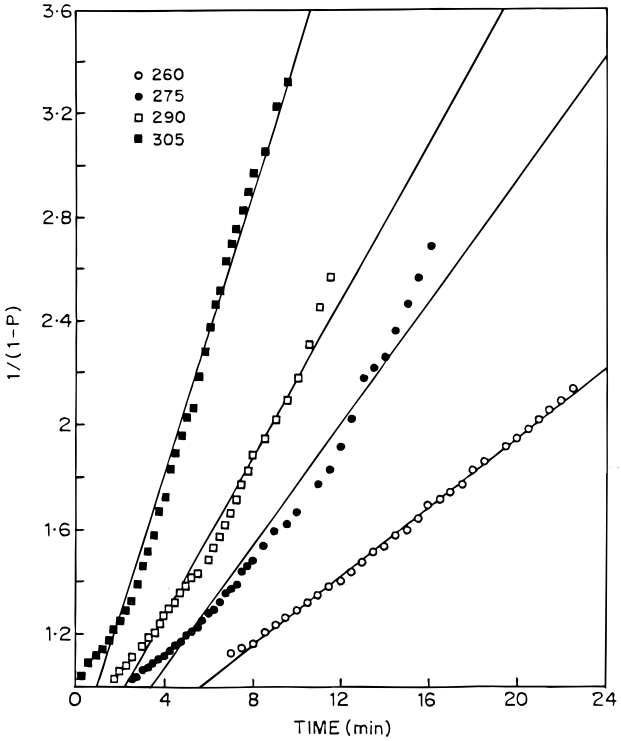

Figure 7. Second-order plot illustrating effect of temperature for catalyzed PET 40/60 (HQDA + TA) reactions.

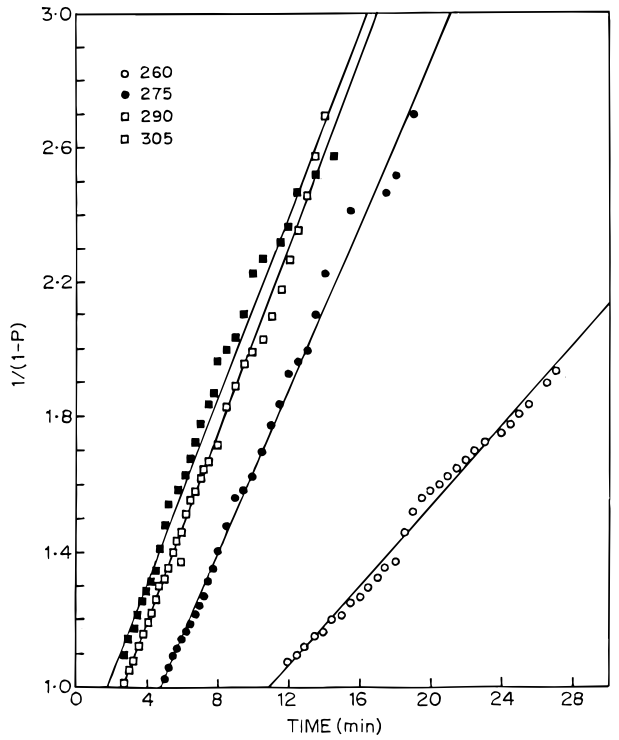

Figure 8. Second-order plot illustrating effect of temperature for catalyzed PET 60/40 (HQDA + TA) reactions.

The Arrhenius plots for the three-component copolyesterification as a function of composition are given in Figures 9−12. The plots suggest that the catalyst plays a marginal role in enhancing the reaction rate. A look at Table 1 indicates that the energy of activation values for a few runs are larger than those for the corresponding uncatalyzed reactions. The rate constants for the catalyzed reactions are numerically similar.

More Complex Kinetic Model. The major reactions depicted in Figure 1 can be represented by eqs I−VII. As indicated earlier, reaction schemes IV and V are considered only to show how larger blocks of TH units are inserted into the PET chain. These reactions are feasible only if the concentrations of HQDA and TA are in excess of 67%. Reaction events IV and V are equivalent to reactions II and III, respectively. Details of these equations have already been discussed in a previous section. Therefore, reactions I−III, VI, and VII are the dominant reactions. There are two possible pathways through which the TH unit can be inserted into the PET chain, as discussed earlier. These two mechanisms are based on the combination of eqs I, II,

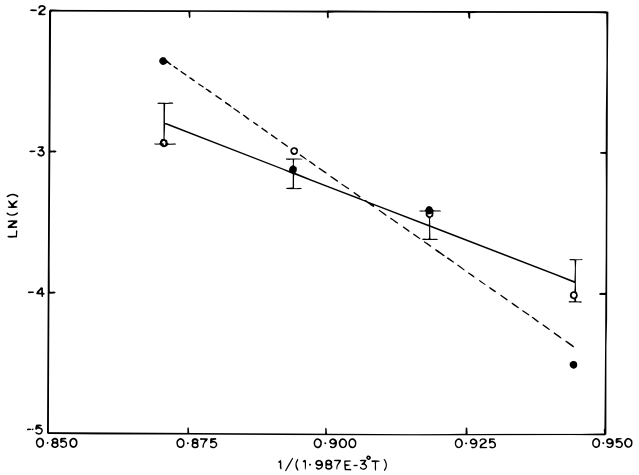

Figure 9. Arrhenius plot for uncatalyzed and catalyzed PET 30/70 (HQDA + TA) reactions. Dashed and solid lines represent least-squares fit for catalyzed and uncatalyzed reactions, respectively. The error bars for the uncatalyzed reactions are only shown for clarity.

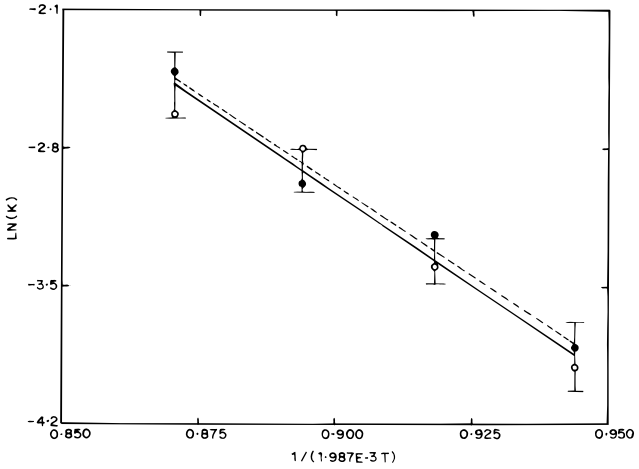

Figure 10. Arrhenius plot for uncatalyzed and catalyzed PET 40/60 (HQDA + TA) reactions. Dashed and solid lines represent least-squares fit for catalyzed and uncatalyzed reactions, respectively. The error bars for the uncatalyzed reactions are only shown for clarity.

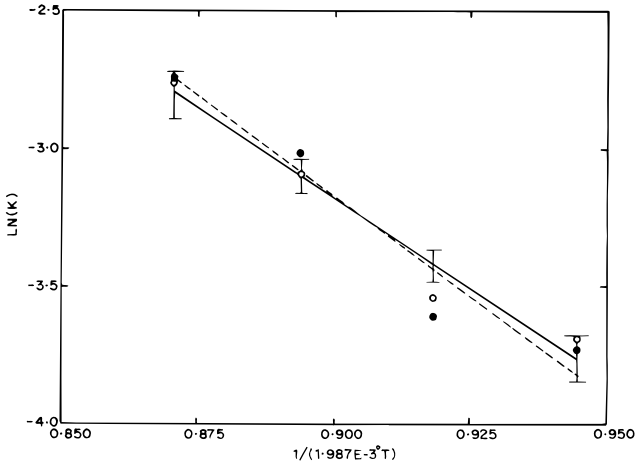

Figure 11. Arrhenius plot for uncatalyzed and catalyzed PET 50/50 (HQDA + TA) reactions. Dashed and solid lines represent least-squares fit for catalyzed and uncatalyzed reactions, respectively. The error bars for the uncatalyzed reactions are only shown for clarity.

and III and eqs VI, VII, and III, respectively. A more complex kinetic model is developed on the basis of eqs I−III, VI, and VII.

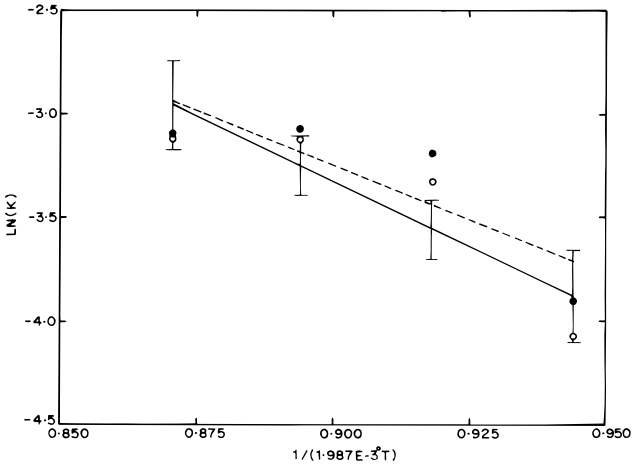

Figure 12. Arrhenius plot for uncatalyzed and catalyzed PET 60/40 (HQDA + TA) reactions. Dashed and solid lines represent least-squares fit for catalyzed and uncatalyzed reactions, respectively. The error bars for the uncatalyzed reactions are only shown for clarity.

Rates of formation of segment $S_{PET}T$, segment $S_{PET}TH$, dimer HT, and acetic acid are given by eqs 9, 10, 11, and 12, respectively.

$$\frac{d[P_1]}{dt} = k_{s_1}[PET][T] - k_{e_1}[P_1][H] - k_{c_1}[P_1][P_2] + k_{s_2}[PET][HT] \quad (9)$$

$$\frac{d[P_2]}{dt} = k_{e_1}[P_1][H] - k_{c_1}[P_1][P_2] + k_{s_2}[PET][HT] \quad (10)$$

$$\frac{d[HT]}{dt} = k_h[H][T] - k_{s_2}[PET][HT] \quad (11)$$

$$\frac{d[CH_3COOH]}{dt} = k_{e_1}[P_1][H] + k_{c_1}[P_1][P_2] + k_h[H][T] \quad (12)$$

where $P_1 = S_{PET}T$ and $P_2 = S_{PET}TH$. Subtracting eq 10 from eq 9, we get

$$k_{s_1}[PET][T] - 2k_{e_1}[P_1][H] = 0$$

$$\left(\frac{k_{s_1}}{2}\right)[PET][T] = k_{e_1}[P_1][H] \quad (13)$$

Adding $2k_{c_1}[P_1][P_2]$ to both sides of eq 10, we get

$$2k_{c_1}[P_1][P_2] + \frac{d[P_2]}{dt} = k_{e_1}[P_1][H] - k_{c_1}[P_1][P_2] + 2k_{c_1}[P_1][P_2] + k_{s_2}[PET][HT] = k_{e_1}[P_1][H] + k_{c_1}[P_1][P_2] + k_{s_2}[PET][HT] \quad (14)$$

At steady state

$$\frac{d[HT]}{dt} = k_h[H][T] - k_{s_2}[PET][HT] = 0$$

$$k_h[H][T] = k_{s_2}[PET][HT]$$

Substituting this into eq 14, we get

$$2k_{c_1}[P_1][P_2] + \frac{d[P_2]}{dt} = k_{e_1}[P_1][H] + k_{c_1}[P_1][P_2] + k_h[H][T] \quad (15)$$

The right-hand side of eq 15 is equal to d[CH_3COOH]/dt. Therefore

$$\frac{d[CH_3COOH]}{dt} = \frac{d[P_2]}{dt} + 2k_{c_1}[P_1][P_2] \qquad (16)$$

At steady state, d[P_2]/dt = 0. Therefore

$$\frac{d[CH_3COOH]}{dt} = 2k_{c_1}[P_1][P_2] \qquad (17)$$

Similarly, by adding eqs 9 and 10, we get

$$\frac{d[P_1]}{dt} + \frac{d[P_2]}{dt} = k_{s_1}[PET][T] - k_{e_1}[P_1][H] - k_{c_1}[P_1][P_2] + k_{s_2}[PET][HT] + k_{e_1}[P_1][H] - k_{c_1}[P_1][P_2] + k_{s_2}[PET][HT]$$

$$\frac{d[P_1]}{dt} + \frac{d[P_2]}{dt} = k_{s_1}[PET][T] - 2k_{c_1}[P_1][P_2] + 2k_{s_2}[PET][HT] \qquad (18)$$

At steady state, d[P_1]/dt + d[P_2]/dt = 0,

$$k_{s_1}[PET][T] - 2k_{c_1}[P_1][P_2] + 2k_{s_2}[PET][HT] = 0$$

$$2k_{c_1}[P_1][P_2] = k_{s_1}[PET][T] + 2k_{s_2}[PET][HT] = \frac{d[CH_3COOH]}{dt}$$

$$\frac{d[CH_3COOH]}{dt} = -\frac{d[H]}{dt} = k_{s_1}[PET][T] + 2k_h[H][T] \qquad (19)$$

On the other hand, the rate of disappearance of PET is given by eq 20

$$-\frac{d[PET]}{dt} = k_{s_1}[PET][T] + k_{s_2}[PET][HT] \qquad (20)$$

Dividing eq 20 by eq 19 so as to eliminate time results in the following functional relation between HQDA and PET:

$$\frac{d[PET]}{d[H]} = \frac{k_{s_1}[PET][T] + k_h[H][T]}{k_{s_1}[PET][T] + 2k_h[H][T]}$$

$$\frac{d[PET]}{d[H]} = \frac{[PET][T] + k_r[H][T]}{[PET][T] + 2k_r[H][T]}$$

where $k_r = k_h/k_{s_1}$

$$\frac{d[PET]}{d[H]} = 1 - \frac{k_r[H]}{[PET] + 2k_r[H]} \qquad (21)$$

Equation 21 is independent of TA concentration. In other words, disappearance of PET with respect to HQDA is independent of TA concentration. The number of moles of acetic acid produced is calculated from eqs 19 and 21 by using the Runge−Kutta procedure at various values of k_{s_1} and k_h. The plot of moles of acetic acid produced versus time for the uncatalyzed reaction between PET:(HQDA + TA) [50:50] at three different temperatures is presented in Figure 13. The best fits were obtained at homopolymerization rates 6.05, 7.75, and 11.82 times faster than the PET chain slicing rate

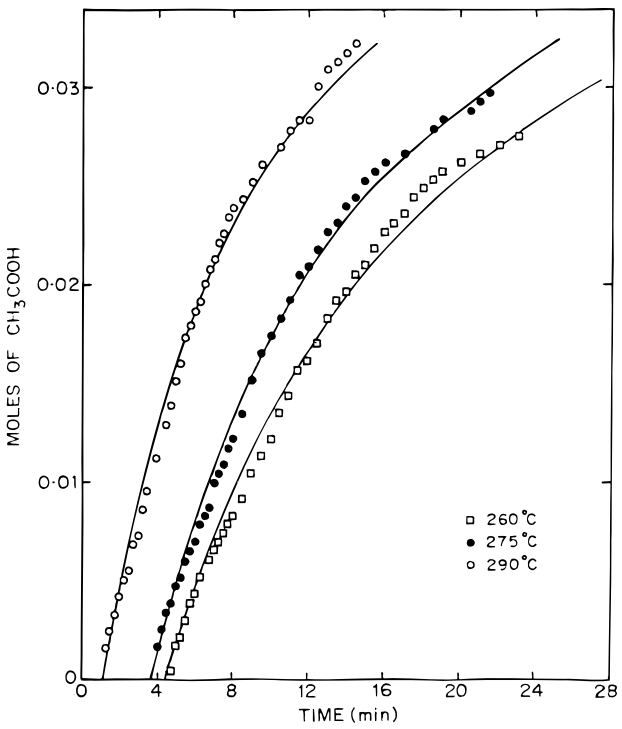

Figure 13. Plot of moles of acetic acid generated versus time for uncatalyzed PET 50/50 (HQDA + TA) reactions.

at 260, 275, and 290 °C, respectively. Since, $k_{s_1} < k_h$, the rate of acetic acid production in eq 19 is given by eq 22.

$$\frac{d[CH_3COOH]}{dt} = 2k_h[H][T] = 2k_h[H]^2 = 2k_h(a - x)^2 \qquad (22)$$

This equation is identical to eq 8, already discussed in the section on a simplified kinetic picture. Similarly, second-order plots of the uncatalyzed reaction between 0.05 mol of PET, 0.025 mol of HQDA, and 0.025 mol of TA are compared in Figure 14. It is clear from the figure that the copolymerization rate is faster than the rate of homopolymerization. In both these experiments, the moles of HQDA and TA are similar. Therefore, acetic acid produced is 0.05 mol in both cases. The ratio of the two rate constants is equivalent to the ratio of the slopes; i.e. copolymer/homopolymer and is close to 2 (1.8). This indirectly validates the steady-state approximation.

Characterization. The HQDA−TA polyesters were heated at 10 °C/min from room temperature to 325 °C, the upper limit of the microscope. The samples were found to be infusible. The PET−HQDA−TA copolyesters were analyzed in a similar manner. Depolarization of light was observed in all copolyesters, PET 30/70 (HQDA + TA) to PET 60/40 (HQDA + TA). The microscopic observations revealed the presence of some nonmelting polyesters in the PET-30 and -40 copolyester compositions.

DSC thermograms of the first and second heating cycles (heating rate: 20 °C/min) for polyesters PET 30/70 (HQDA + TA) to PET 60/40 (HQDA + TA) are shown in Figure 15. The first heating cycle consisted of heating the sample to 260 °C at the rate of 20 °C/min. The sample was then cooled to 50 °C at a cooling rate of 20 °C/min and reheated in the second heating cycle to 460 °C at 20 °C/min.

The thermodynamic parameters pertinent to the first and second heating cycles are presented in Table 2.

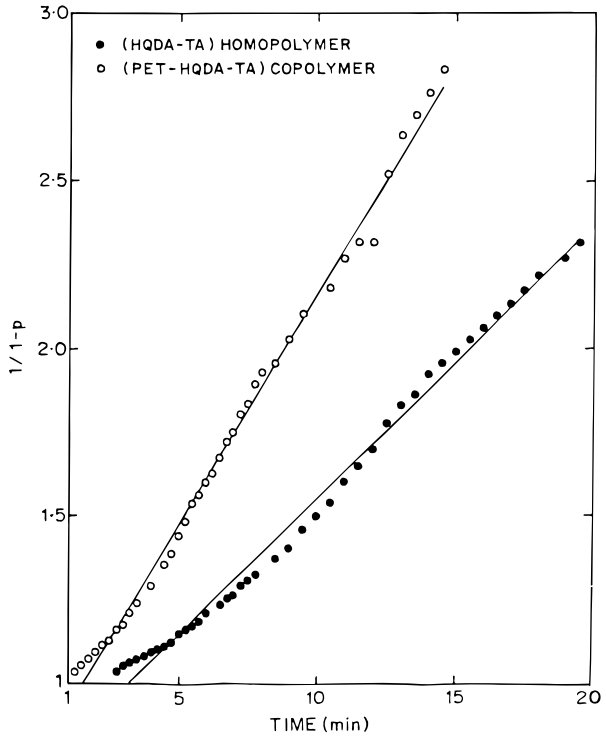

Figure 14. Comparison of homopolyesterification and copolyesterification reactions carried out at 290 °C.

The entities present in the copolyester can be depicted by the following global structure:

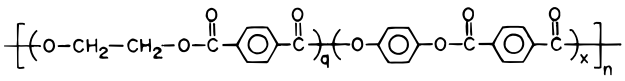

Here q and x represent the mole percent of PET and HQDA + TA units along the chain. At 50 mol % of HQDA + TA, the structures would resemble a rigid rod−flexible spacer type thermotropic system consisting of a triad mesogen with carboxylic groups coupled to 1,2-ethanediol. At lower (<50) mole percent of HQDA + TA, the mesogen is diluted at the cost of PET moieties.

Above 50 mol % of HQDA + TA in the copolyester, the averaged mesogen length would increase while the flexible spacer will remain unchanged and consist of dimethylene units of 1,2-ethanediol. At sufficiently high (>60) mole percent of HQDA + TA, the averaged mesogen formed is nonmelting and the thermotropic character disappears.

The PET−OB and PET−HQDA−TA copolyesters of similar composition differ marginally in their structures. The direction of the ester linkages along the copolyester chain is altered. This change is known to alter the packing and crystal structure details.[26]

Microscopic observations made in the temperature range over which the first-order transitions were noted in the DSC revealed phase changes. Optical anisotropy was noted for all the samples. The PET−HQDA−TA system exhibits higher melting temperatures as compared to the PET−OB system of similar composition. The melting temperatures are lower than the isothermal polymerization temperatures. Thus, the copolymers would possess a randomized sequence of PET and HQDA−TA.[27]

The melting temperatures reported in Table 2 in conjunction with optical microscopic observations revealed that the melting transitions are liquid crystalline.

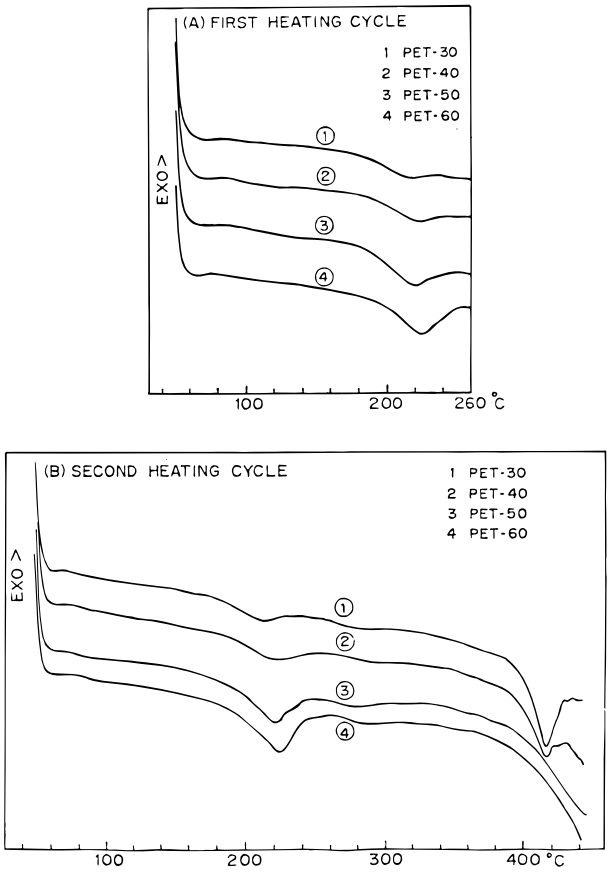

Figure 15. DSC endotherms for uncatalyzed PET−HQDA−TA systems at 305 °C: (a) first heating cycle; (b) second heating cycle.

Table 2. Transition Temperatures and Thermodynamic Data of Catalyzed and Uncatalyzed Reactions[a]

comp (mol %)	T_{m1} (°C)	ΔH_{m1} (kJ/mol)	T_{m2} (°C)	ΔH_{m2} (kJ/mol)
PET 30/70 (HQDA + TA)	213	1.9	213	1.7
PET 40/60 (HQDA + TA)	219	3.3	221	3.4
PET 50/50 (HQDA + TA)	216	7.2	221	8.2
PET 60/40 (HQDA + TA)	223	9.85	223	10.4

[a] Reaction temperature 305 °C; reaction time 1 h. T_{m1} = melting temperature (first heating cycle); T_{m2} = melting temperature (second heating cycle); ΔH_{m1} = enthalpy of melting (first heating cycle); ΔH_{m2} = enthalpy of melting (second heating cycle).

Extraction with *m*-cresol:1,1,2,2-tetrachloroethane 60/40 v/v at the end of the reaction did not yield unreacted PET. It is thus obvious that the existence of unreacted PET at the end of reaction is remote. Thermal analysis of a typical PET 60/40 (HQDA + TA) sample by quench cooling the melt to −25 °C and reheating at a rate of 20 °C/min did not reveal a T_g or cold crystallization peak corresponding to PET.

The PET−HQDA−TA copolyesters exhibited higher enthalpy values when compared to PET−OB systems of similar composition.[21] The highest enthalpy value is noted for PET 60/40 (HQDA + TA) and is of the order of 10.4 kJ/mol. Within the copolyester series, the degree of crystallinity increases with rise in PET content. These progressively increasing values of ΔH_{m_1} and ΔH_{m_2} can be correlated to the meltable fractions of the copolyester. A rise in ΔH_{m_2} values is noted on comparing the enthalpy values of the first and second heating cycles. This could plausibly be due to continued polycondensation reactions and alterations in the crystallite size.

Conclusions

The kinetics of a three-component PET−HQDA−TA system in melt polyesterification have been analyzed. The kinetic analysis was expected to be complex due to the possibility of several reactions occurring in parallel. However, the following plausible assumptions were made to make the analysis tractable. HQDA and TA combine to form a dimer, producing acetic acid as a byproduct. This dimer slices the PET chain to form segments $S_{PET}T$ and $S_{PET}TH$. The coupling of these segments results in the insertion of the hydroquinone−terephthalate unit into the PET chain. To retain the simplicity of analysis, a key assumption was made to the effect that acetic acid is produced through only two channels: (i) HQDA and TA reacting to form dimer and (ii) this dimer subsequently inserted into the PET chain. Kinetically, both these reactions were assumed and shown to be of second order with respect to the reactants. In the second reaction, the concentrations of PET repeat units and the dimer figure as a product. Even though in principle other reactions can also give rise to acetic acid like dimer reacting with HQDA or TA, the probabilities for these processes are small in comparison to the main reaction postulated above.

Trans−trans esterification involving ester units buried within the oligomeric chain from HQDA and TA can also react, but without giving rise to acetic acid. These reactions are extremely slow and hence assumed to be too slow to be of any consequence in the overall mass balance. The reaction network involves a second-order reaction for which analytical expressions are not possible. The two progress variables for dimerization and copolyesterification can be compared to give one net rate expression for the acetic acid production. A more complex mechanistic model also reduces to the simplified rate model if we bring in the steady-state approximation.

One remarkable finding was that, if the assumption is made that the second-order reaction involving HQDA and TA to form a dimer is much slower than the rate of incorporation of the dimer into PET, a steady-state approximation can be safely applied to the production of dimers, as is the standard practice in the literature. The net rate of production of the dimer is thus set equal to zero. The overall production rate of the acetic acid will be twice that of the rate of production of homopolyester. Under steady-state conditions this also will be equal to twice the rate of production of the dimer of HQDA−TA. One conclusion immediately obvious is that the rate of acetic acid production should obey a neat second-order plot. A plot of $1/(1 - p)$ against time should generate a linear fit. Here, p denotes the fractional conversion where HQDA and TA have the same stoichiometric conversions. This kinetic order should be independent of the starting concentration of PET. The rate constant for the dimerization steps is determined independently. The numerical value of the rate constant in the presence of PET is equal to twice that of the HQDA and TA reactions. One cannot offer a concrete explanation for the lowering of rate constants (observation of less than the stipulated doubling of the rate constants). We only speculate that it may have something to do with viscosity effects prevalent in a molten system. Arrhenius plots reveal that the catalyst has a marginal role to play.

Microscopic observations revealed that the polycondensate of HQDA and TA is nonmelting. The copolyesters PET 30/70 (HQDA + TA) to PET 60/40 (HQDA + TA) are liquid crystalline.

The first-order transition temperature values obtained from DSC, in conjunction with microscopic observations, revealed the liquid crystalline nature of these materials. The increasing values of the enthalpy of fusion indicated an increase in the crystalline content of the copolyester due to formation of copolyesters of PET−HQDA−TA and the absence of nonmelting HQDA−TA polyester.

Acknowledgment. This work was supported by funding from the New Fibres and Composites Program, Department of Science and Technology, New Delhi. The authors are obliged to Miss B. Gokhale for the experimental help provided during the course of this work.

References and Notes

(1) Ober, C.; Lenz, R. W.; Galli, G.; Chiellini, E. *Macromolecules* **1983**, *16*, 1034.
(2) Chen, G.; Lenz, R. W. *J. Polym. Sci., Polym. Chem. Ed.* **1984**, *22*, 3189.
(3) Meurisse, P.; Noel, C.; Monnerie, L.; Fayolle, B. *Br. Polym. J.* **1981**, *13*, 55.
(4) Iimura K.; Koide, N.; Ohta, R. *Rep. Prog. Polym. Phys. Jpn.* **1981**, *24*, 231.
(5) Griffin, A. C.; Havens, S. J. *J. Polym. Sci., Polym. Chem. Ed.* **1981**, *19*, 951.
(6) Strzelecki, I.; Liebert, L. *Eur. Polym. J.* **1981**, *15*, 1271.
(7) Roviello, A.; Sirigu, A. *Eur. Polym. J.* **1981**, *15*, 423.
(8) Roviello, A.; Sirigu, A. *J. Polym. Sci., Polym. Lett. Ed.* **1975**, *13*, 455.
(9) Jackson, W. J., Jr.; Kuhfuss, H. F. *J. Polym. Sci., Polym. Chem. Ed.* **1976**, *14*, 2043.
(10) Jackson, W. J., Jr. *Contemp. Top. Polym. Sci.* **1984**, *5*, 117.
(11) Jackson, W. J., Jr. *Br. Polym. J.* **1980**, *12*, 153.
(12) Kwolek, S. L.; Luise, R. R. *Macromolecules* **1976**, *19*, 1789.
(13) Krigbaum, W. R.; Hakemi, H.; Kotek, R. *Macromolecules* **1985**, *18*, 965.
(14) Sinta, R.; Gaudiana, R. A.; Minns, R. A.; Roges, H. G. *Macromolecules* **1987**, *20*, 2374.
(15) Griffin, B. P.; Cox, M. K. *Br. Polym. J.* **1980**, *12*, 147.
(16) Goodman, I.; McIntyre, J. E.; Stimpson, J. W. *British Patent* 989,552, 1965; U.S. Patent 3,321,437, 1967.
(17) Goodman, I.; McIntyre, J. E.; Alfred, D. H. *British Patent* 993,272, 1965; U.S. Patent 3,368,998, 1967.
(18) Kuhfuss, H. F.; Jackson, W. J., Jr. U.S. Patent 3,778,410, 1973; U.S. Patent 3,804,805, 1974.
(19) Schaefgen, J. R. U.S. Patent 4,075,262, 1978.
(20) Hamb, F. L. *J. Polym. Sci., Polym. Chem. Ed.* **1972**, *10*, 3217.
(21) Mathew, J.; Ghadage, R. S.; Prasad, S. D.; Ponrathnam, S. *Macromolecules* **1994**, *27*, 4021.
(22) Mathew, J.; Bahulekar, R. S.; Ghadage, R. S.; Ponrathnam, S.; Prasad, S. D. *Macromolecules* **1992**, *25*, 7338.
(23) Kricheldorf, H. R.; Schwarz, G. *Makromol. Chem.* **1983**, *184*, 475.
(24) Flory, P. J. *Chem. Rev.* **1946**, *39*, 169.
(25) Aris, R. *The Mathematical Theory of Diffusion and Reaction in Permeable Catalysts*; Clarendon Press: Oxford, 1975; Vol. 1, p 104.
(26) Ober, C. K.; Bluhm, T. L. *Curr. Top. Polym. Sci.* **1987**, *1*, 249.
(27) Jin, J. I. Thermotropic Aromatic Polyesters Having Ordered Comonomer Sequence. In Weiss, R. A., Ober, C. K., Eds.; *Liquid Crystalline Polymers*; ACS Symposium Series 435; American Chemical Society: Washington, DC, 1990; pp 33−45.

MA950842W